



The Effect of Mechanical Recycling on the Thermal, Mechanical, and Chemical Properties of Poly (Butylene Adipate-Co-Terephthalate) (PBAT), Poly (Butylene Succinate) (PBS), Poly (Lactic Acid) (PLA), PBAT-PBS Blend and PBAT-TPS Biocomposite

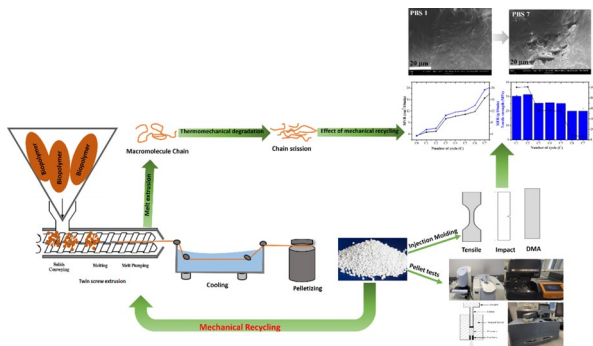
Nomvuyo Nomadolo^{1,2} · Asanda Mtibe¹ · Osei Ofosu^{1,3} · Caroline Mekoa¹ · John Letwaba¹ · Sudhakar Muniyasamy^{1,2}

Accepted: 4 December 2023
© The Author(s) 2024

Abstract

Mechanical recycling of plastics is regarded as the best option to minimize plastic waste pollution in the environment as it is well established and offers valorisation of plastics; however, there is limited research on the mechanical recyclability of biopolymers. This work aimed to evaluate the effect of multiple reprocessing on the mechanical, thermal, physical, chemical, and morphological properties of poly (butylene adipate-co-terephthalate) (PBAT), poly (butylene succinate) (PBS), poly (lactic acid) (PLA), PBAT-PBS blend, and PBAT-thermoplastic starch (TPS) composite. Low-density polyethylene (LDPE), a conventional non-biodegradable plastic, was also reprocessed for comparison studies. The biopolymers were extruded seven times in a twin-screw extruder and injection moulded into test specimens. Their properties were investigated at each extrusion cycle. Tensile, impact strength, and melt flow index (MFI) results of neat PBAT and PBAT-TPS were stable with slight changes throughout the seven reprocessing cycles and were comparable to LDPE. The properties of PBS, PLA, and PBAT-PBS blend, on the other hand, started to decrease after the second melt extrusion cycle. In addition, differential scanning calorimetry (DSC), thermogravimetry (TGA), and dynamic mechanical analysis (DMA) results showed that LDPE, PBAT, and PBAT-TPS exhibited better thermal and mechanical stability as compared to PBS, PLA, and PBAT-PBS blend. The FTIR spectroscopy results showed that the characteristic peaks of C=O and C-O around 1710 cm^{-1} and $1046\text{--}1100\text{ cm}^{-1}$ for PBS, PLA, and PBAT-PBS decreased due to multiple thermal processing, while those of PBAT and PBAT-TPS were unaffected. Scanning electron microscopy (SEM) micrographs of the fractured cross-sectional surface of PBS, PLA, and PBAT-PBS tensile specimens clearly evidenced the degradation of the biopolymers by severely fractured morphology as a result multiple reprocessing cycle. The results demonstrate that the fully biodegradable PBAT and PBAT-TPS can be mechanically recycled for at least seven cycles, and therefore, the service life of biodegradable polymers can be extended, and it is comparable with petroleum-based plastic.

Graphical Abstract



Extended author information available on the last page of the article

Keywords Biopolymers · Blends · Melt extrusion · Mechanical recycling · Degradation

Introduction

There has been a global drive towards developing biopolymers as an alternative to petroleum-based polymers to mitigate fossil resources and post-consumer plastic disposal issues. These issues include the depletion of petroleum resources, the emissions of greenhouse gases, as well as plastic pollution. As a result, the production of biopolymers has considerably increased in the last decade since it uses less fossil fuels and the biopolymers can biodegrade into carbon dioxide and water when discarded, thus reducing their carbon footprint. *Biopolymers* are plastics that are biobased or biodegradable or can be both [1–4]. Over 2.4 million tons of biopolymers are produced globally, with the packaging sector engrossing the most significant share of about 60% [5, 6]. The recent European biopolymers report shows that PBAT, PLA, starch-based polymer blends, and PBS are the largest biopolymers produced at 19.2%, 18.9%, 16.4%, and 3.4% global production capacity, respectively. Additionally, this global production is expected to double in less than five years due to the rising demand for biopolymers [7, 8]. Consequently, after the end of service life, biopolymers will likely end up in plastic waste streams with conventional petroleum-based polymers. While attention has been on developing and optimizing various biopolymers to meet the standard performance characteristics of existing conventional polymers for various applications, the recyclability of biopolymers remains largely unexplored. To date, biopolymers have not been methodically integrated into the waste management system, and the substantial growth necessitates that researchers, society, and industry address biopolymer recycling for process and post-consumer waste at an early stage.

The European regulations on plastic waste management assert that waste management should follow a clear hierarchy to indicate a priority order in the policy and legislation for waste management and prevention [6]. The primary priority for non-biodegradable and biodegradable plastics is mechanical recycling. Mechanical recycling allows the preservation of polymers and material value by reprocessing into secondary products in contrast to other waste management methods such as energy recovery, chemical recycling, and composting. Additionally, mechanical recycling has a well-established infrastructure worldwide; it is relatively simple and requires low investment. Its technical parameters are controlled, providing ease of preparation [9–12]. To this point, assessments of the effect of reprocessing on the properties of the biopolymers during mechanical recycling are

necessary to determine the quality of recyclates and guarantee their further performance in second-market applications. Generally, mechanical recycling involves sorting, grinding, and conventional polymer processing methods to make recycled plastics. The recycled plastics may have downgraded properties compared to virgin plastics due to processing temperature, mechanical shear stress, and the presence of oxygen [13–17]. In certain applications, recycled plastics are amalgamated with virgin plastic to circularize the recycled plastics, reducing the cost, and eliminating the plastic waste issues. For example, European plastics producers targets 30% of recycled plastic incorporation into packaging plastic by 2030 [18]. Similarly, many countries have adopted legislation regulating plastic waste to prevent, reduce, and control pollution in landfills and marine environments by dumping [18, 19]. Much research is required to study the effect of multiple extrusion processes on biopolymers, which is imperative as it informs the melt-processing stability of the biopolymers and will therefore inform their integration into existing recycling infrastructure [13, 20–23].

To the best of our understanding, minimal work on the effect of mechanical recyclability and the mechanistic degradation behaviors of biopolymers has been disseminated [18]. *Oliveira et al.* [20] evaluated the effect of PBAT on the thermal and mechanical properties of the polypropylene (PP)/PBAT-thermoplastic starch (TPS) blend, which was prepared via a single extrusion process and subjected to seven reprocessing cycles. The authors suggested that the repeated shearing stress at elevated temperatures weakened the PP chain resulting in the rapturing of the polymer via the chain scission mechanism; interestingly, PBAT enhanced the yield stress, elastic modulus, and thermal stability of the blend. On the other hand, *Resch-Fauster and co-workers* [21] suggested that repeated processing might lead to hydrolytic degradation of PBAT instead of poly (3-hydroxybutyrate-co-3-hydroxyvalerate) (PHBV) in the PHBV/PBAT blend during the multiple extrusion cycles reprocessing. *Georgousopolou et al.* [13] and *Resch-Fauster et al.* [21] evaluated the mechanical recycling of PBS using extrusion over seven reprocessing cycles. The authors report a severe increase in melt flow index (MFI) due to polymer degradation. *Georgousopolou et al.* [13] suggested that the high shear forces caused the branching and recombination reaction as evidenced by the increase in molecular weight M_w and the increase in crystallinity, X_c . *Resch-Fauster et al.* [21] proposed hydrolysis as the prevailing mechanism evidenced by the increase in M_w and decrease in X_c . *Bourmaud et al.* [24] assessed blending PBS with PLA to

improve the melt-processing stability during reprocessing up to seven injection molding cycles. The authors report that the blend's Young Modulus and strength-at-break were unaffected by reprocessing; however, the impact strength and elongation-at-break were greatly affected after the first cycle. Blending PBS with other biopolymers might stabilize the melt processability of PBS, prompting more improvement. Interest in the recyclability of biopolymers has been mostly directed toward PLA, with the significant outcome detailing that PLA is susceptible to thermomechanical degradation, evidenced by the decrease in molecular weight, M_w , mechanical properties, and the increase in MFI from the fifth melt-extrusion cycle [19, 25–27]. Citing hydrolysis of PLA as the primary cause of chain scission degradation, which ultimately leads to the deterioration of its properties [23, 28, 29]. The assessment of PLA recyclates has revealed that elongation deformation, shear stress, and heat also promote homolytic chain rupture and intermolecular transesterification mechanisms, which further enhance the thermal degradation of the polymer [23].

This present study evaluates a systematic approach similar to industrial mechanical recycling by multiple extrusion processing of biopolymers, biopolymer blend, and biocomposite up to seven cycles. After each processing cycle, the effect of thermal, mechanical, structural, and morphological properties of PBAT, PBS, PBAT-PBS (50/50, wt%) blends, and PBAT-TPS (70/30, wt%) were characterized by tensile, impact, MFI, DMA, TGA, DSC, FT-IR and SEM analyses. After reprocessing, the relationship between the biopolymer and their physical, chemical, and thermal properties was generated.

Materials and Experimental Procedures

Material Description, Sample Preparation, and Multiple Extrusion

Materials

PBAT Ecoflex C1200 grade was purchased from BASF, South Africa, PBS FZ91 grade was purchased from PTT-MCC Biochem, Thailand and PLA LX175 grade was purchased from Total Corbion. Soy meal starch was obtained from RCL Foods South Africa, for preparing thermoplastic starch (TPS).

Preparation of thermoplastic starch (TPS)

The preparation of the TPS master batch from soy meal starch was carried out in a two-step process. In the first step, 15phr Urea was mixed with 25phr water using a mixer, followed by the addition of 30% glycerol. After 30 min of

stirring, the mixture was stored overnight at room temperature for denaturing. In the second step, the denaturized starch mixture was melt-extruded into TPS using a twin screw extruder (TE-30/600-11-40, Extrusion Machinery Co., Ltd, China) at 120 °C. The extruded TPS strand was pelletized into granules and then dried at 80 °C for 8 h in a ventilated oven. After drying, the TPS was kept in a vacuum-sealed bag and stored dry.

Preparation of Biopolymer Blends and Composite

Before processing PBAT-PBS blends and PBAT-TPS, each material was pre-dried in a ventilated oven at 80 °C for 8 h. PBAT-PBS (50/50 wt%) and PBAT-TPS (70/30 wt%) were prepared in a melt extrusion processing at optimized temperatures between 120 and 160 °C using a co-rotating twin-screw extruder (TE-30/600-11-40, Extrusion Machinery Co., Ltd, China). This was followed by a palletization process, and the pellets were then dried in a ventilated oven at 80 °C for 8 h.

Mechanical Recycling Processing

LDPE, PBAT, PBS, PLA, PBAT-PBS, and PBAT-TPS pellets were pre-dried in a ventilated oven at 80 °C for 8 h. The polymers and their blends were processed using a co-rotating twin-screw extruder (TE-30/600-11-40, Extrusion Machinery Co., Ltd, China). The temperature profiles of the extruder varied from 120 to 180 °C, from the feeding to the die zone. This was followed by quenching in a water tank, then pelletized and dried in a ventilated oven for 8 h at 80 °C. The resultant pellets were characterized by MFI, DSC, and TGA. For each cycle, the extruded pellets were injection molded (e-mac50, ENGEL AUSTRIA GmbH, Austria) to produce test specimens. The temperature profile was optimized from feeding to nozzle at 130–180 °C. The injection molded specimens were cooled to room temperature for 24 h and then characterized for tensile, Impact, DMA, and SEM. This process was repeated seven times for each polymer with the exception of biopolymer that lost melt strength at the sixth cycle and were difficult to process.

Characterization

Tensile

An Instron universal testing machine, model 5966 (Instron, Norwood, MA, USA), was used to investigate tensile properties of neat biopolymers, (PBAT, PBS, PLA), biopolymer blend PBAT-PBS, PBAT-TPS biocomposite, and petroleum-based polymer (LDPE). Five tensile specimens for each sample were tested according to ASTM D638.

Impact

The impact strength tests were performed according to the ASTM D256 standard using a Ceast-Resil-Impactor instrument operated with a 15 J hammer at a speed of 3.68 m/s. Tests were done on notched specimens with 8 cm by 4 cm, width and thickness, respectively. The impact strength of the samples was calculated in joules per square meter (J/m^2) with standard deviations of six independent tests.

Melt Flow Index (MFI)

The melt mass-flow rates (MFR) and melt volume-flow rate (MVR), were determined according to ISO 1133 in an MFI equipment from (Multiweight), CEAST using a 1 mm diameter nozzle at a temperature of 160 °C and a mass of 2.16 kg. The MFR and MVR were recorded in $cm^3/10min$ and $g/10 min$, respectively.

Differential Scanning Calorimetry

Approximately 5–10 mg of polymer samples were weighed and analyzed in the temperature range of –40 to 200 °C under a nitrogen atmosphere using DSC-8500 (PerkinElmer, Branford, CT, USA) for the determination of the melting and cold crystallization temperatures, as well as their corresponding enthalpies (ΔH 's). Each sample underwent three successive scans of heating, cooling, and heating at a rate of 10 °C/min. The degree of crystallinity (X_c) was calculated using Eq. 1 where the enthalpy of 100% crystalline PBAT (ΔH_{m100}), 100% crystalline PLA (ΔH_{m100}) and 100% crystalline PBS (ΔH_{m100}) were taken as 114 J/g, 93.7 J/g and 110 J/g respectively [30, 31].

$$X_c = \frac{\Delta H_m}{\Delta H_{m100}} \times 100 \quad (1)$$

Thermogravimetric Analysis

A thermogravimetric analyzer (TGA), Pyris (PerkinElmer) 5500, was used to analyse the thermal degradation behaviour of the test samples between 30 and 700 °C at a heating rate of 10 °C/min under a nitrogen atmosphere.

Dynamic Mechanical Analysis

The viscoelastic behavior of the biopolymers was examined by dynamical mechanical measurements (DMA) 8000 (PerkinElmer Inc., Ohio, OH, USA). ASTM D4065-06 (2006) standard test method was employed to measure the storage modulus (E'), and loss factor ($\tan \delta$) at a frequency of

10 Hz. The dynamic mechanical analysis was performed at a temperature range between –40 and 100 °C, with a strain factor and ramp rate of 0.3704 and 5 °C/min, respectively.

Fourier Transform Infrared Spectroscopy

To examine the chemical structures of the test granules, attenuated total reflectance Fourier transform infrared (FTIR) spectroscopy was performed using a PerkinElmer Spectrum 100 spectrometer. The wavelength ranging from 600 to 4000 cm^{-1} was used at a resolution of 4 cm^{-1} with 32 scans.

Scanning Electron Microscopy

To investigate the effect of reprocessing on the morphology of the samples, scanning electron microscopy (SEM), Zeiss Gemini 2 Crossbeam 540 FEG SEM, was employed to image the cross-sectional area of tensile fractured specimens of LDPE, PBAT, PBS, PLA, PBAT-PBS and PBAT-TPS. The fractured specimen was sputter-coated with carbon for two minutes, to allow better electron flow at an accelerated voltage of 2.00 kV.

Results and Discussion

Tensile Properties of neat Biopolymers, their Blend, and Composite

To assess the industrial possibility of recycling biopolymers, their mechanical properties must remain similar over several processing cycles. The tensile strength and strain-at-break plots of LDPE, PBAT, PBS, PLA, PBAT-PBS blend, and PBAT-TPS biocomposite with respect to reprocessing cycles are shown by Fig. 1. The tensile strength and strain-at-break curves of PBAT (Fig. 1b) indicated that the material had a steady tensile strength and strain-at-break throughout the seven reprocessing cycles. This suggests that the biopolymer has high thermomechanical resistance, which may be attributed to the terephthalate content of the PBAT [23, 32, 33]. The results confirm that PBAT has excellent mechanical properties which are similar to those of LDPE as shown in Fig. 1a. Therefore, PBAT is being considered as a viable alternative to LDPE, offering a wide range of applications and the end-of-life options of mechanical recyclability and biodegradability pathways [34–36]. Furthermore, PBAT shows strain-at-break that is about five times more than LDPE. In the case of PBS, tensile strength was also maintained over the seven reprocessing cycles, having a tensile strength of 35.4 MPa and 31.1 MPa for the first and seventh cycle, respectively as depicted in Fig. 1c. The observations demonstrate that the thermomechanical stress applied during

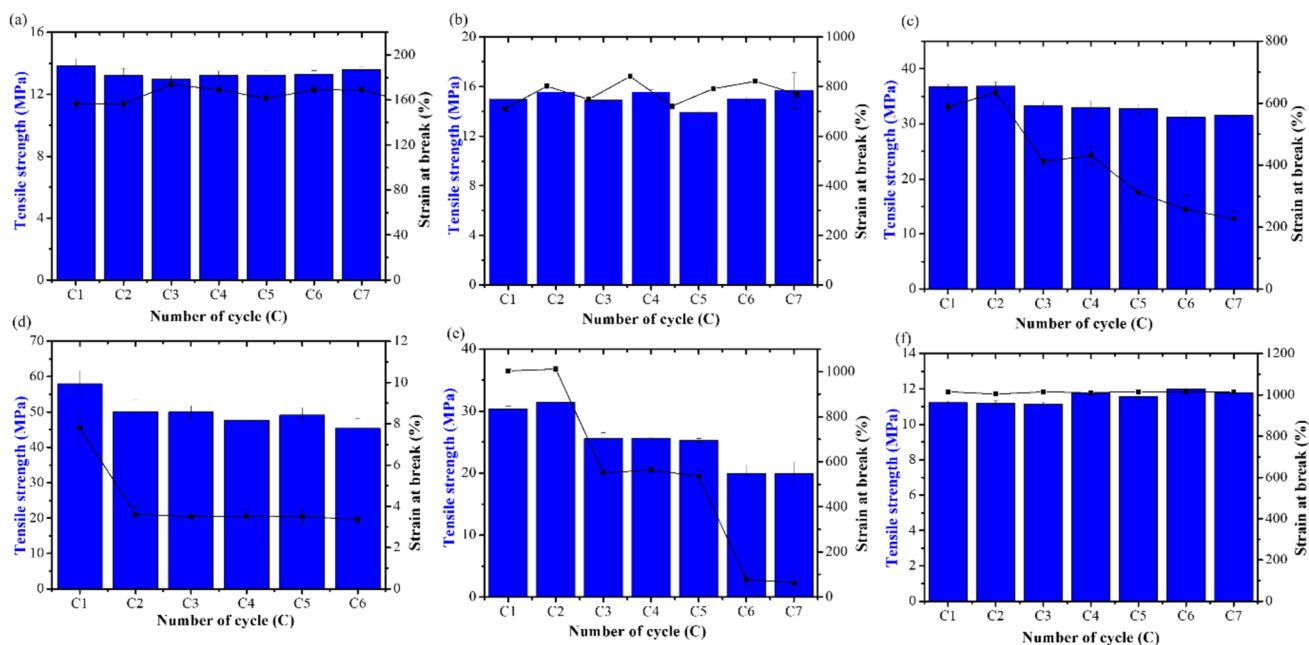


Fig. 1 Tensile strength and strain at break for **a** LDPE, **b** PBAT, **c** PBS, **d** PLA, **e** PBAT-PBS blend, and **f** PBAT-TPS composite subjected to several reprocessing cycles

multiple extrusions of PBS does not change the ability of the material to resist breaking. However, the strain-at-break drastically decreased from 550 to 220%, from the first to the seventh cycle, respectively. The significant decline is attributed to shearing and high temperatures during reprocessing. It has been reported that the thermal and mechanical stress applied during reprocessing cycles results in polymer shearing, which changes the morphology of polymers by shortening polymer chains thereby compromising the mechanical properties, leading to thermomechanical degradation. The shortening of polymer chains is evidenced by the increase in the crystallinity, leading to a more brittle polymer [20, 37]. The tensile strength and strain-at-break results of PLA were found to be 58.7 MPa and 8% after the first reprocessing cycle. The low strain-at-break indicates the brittleness of the biopolymer. Multiple reprocessing caused a 10% decrease in the tensile strength by the sixth cycle, while the strain-at-break severely decreased by 44% by the second cycle, illustrating the high sensitivity of PLA towards mechanical recycling (Fig. 1d). In fact, after the sixth cycle, PLA could no longer be reprocessed due to the low melt strength.

The tensile properties of the PBAT-PBS blend are shown in Fig. 1e. The multiple reprocessing cycles significantly affected both the tensile strength and the strain-at-break due to the presence of PBS in the polymer blend. The strain-at-break for the first and seventh cycles decreased from 1013 to 63.9%, respectively. The observation was attributed to the fact that as reprocessing continues, the stress applied on the polymer blend may have caused the components of the

blends to separate thermodynamically, creating voids and ‘weak spots’ on the polymer matrix, resulting in the drastic decline in the overall strain of the blend. Additionally, PBS has a low melting temperature at around 110 °C, thus, it is less thermally stable than PBAT, making the blended polymer susceptible to thermomechanical degradation. After the seventh cycle, the PBAT-PBS blend was not thermally processable in the twin screw extrusion due to poor rheology and melt strength. In the case of PBAT-TPS, no changes were observed in the mechanical properties throughout the seven reprocessing cycles. Interestingly, PBAT-TPS tensile strength results closely resemble neat PBAT, and the strain-at-break remarkably improved compared to neat PBAT throughout the seven reprocessing cycles. These results indicate that the melt blending process has assisted the compatibility between TPS and PBAT on the mechanical properties of the polymer blend (Fig. 1f).

Impact Strength

The impact test of LDPE, PBAT, and PBAT-TPS test specimen exhibited non-break behavior for all reprocessing cycles. In contrast, the impact energy of PLA, PBS, and PBAT-PBS test specimen decreased with increasing reprocessing cycles. LDPE shows constant impact energy in all reprocessing cycles, whereas PBAT showed a slight decrease of 10%. PBS exhibits an impact strength of 31.6 kJ/m to 19.2 kJ/m from the first to the seven-reprocessing cycle, respectively. These results are consistent with those reported

by Oliveira *et al.* [20] when investigating the effect of reprocessing on the degradation of PP/PBAT-thermoplastic starch. The authors attributed the decrease in impact strength to the effect of the multi-reprocessing of polymers, which primarily induces the chain scission of the polymer, and ultimately weakens the entanglement of macromolecules and therefore increases the crystallinity. This behavior makes the material brittle and decreases mechanical properties [20, 38]. Similar behavior was observed for PLA and PBAT-PBS blend, where there was drastic reduction, leading to the breaking behaviors of the notched samples. The results of PBAT-TPS biocomposite indicate a much higher impact strength than the neat PBAT and are unaffected by the multiple melt extrusion cycles, suggesting that reinforcing PBAT with TPS improves the mechanical properties of the biocomposite (Fig. 2f).

Melt Flow Index

The MFR and MVR of LDPE, PBAT, PBS, PLA, PBAT-PBS blend, and PBAT-TPS biocomposite results are illustrated in Fig. 3. The melt flow index (MFI) represents the flowability of the polymer melt under heat and pressure. It indirectly indicates the molecular weight and viscosity of the polymers. For instance, LDPE exhibits very low melt flow rates, unaffected by the multiple mechanical recycling processes (Fig. 3a). This demonstrates that LDPE has a high molecular weight that remains unaffected by multiple processing cycles. The curve of PBAT, depicted in Fig. 3b,

demonstrated slight increases in melt flow rates as reprocessing cycle increased, which agrees with the tensile and impact strength results. Figure 3c represents PBS results, and the graph shows that unprocessed PBS had a low MVR and MFR values, which were significantly affected by the multiple processing cycles that increased to higher values. The results suggest that recycling led to highly branched and low molecular weight polymer [24]. The same phenomena occurred for neat PLA (Fig. 3d), which experienced a higher effect of mechanical recycling.

Figure 3e shows the results of the PBAT-PBS blend and it was observed that the values of MFR and MVR have steadily increased from C1 to C2. Thereafter, C3-C7 sharply increased, showing that the melt flow properties of the blend have drastically changed due to the change in the weight distribution of the material because of branching [24]. Particularly, on the C6 and C7, the blend has completely deteriorated in its melt flow index to a point where the material is no longer extrudable. Blending TPS with PBAT resulted in a slight increase of MFI in comparison to neat PBAT before multiple reprocessing cycle tests (C0). This may be attributed to the presence of TPS in the PBAT matrix, which degrades at higher temperatures ($> 120^{\circ}\text{C}$). Multiple reprocessing caused an increase in the MVR and MFR of biocomposite from $3.7\text{ cm}^3/10\text{ min}$ and $3.9\text{ g}/10\text{ min}$ to $10.8\text{ cm}^3/10\text{ min}$ and $11.0\text{ g}/10\text{ min}$. However, multiple reprocessing resulted in an improved mixture distribution and dispersion between the TPS and the polymer matrix as a result of reduced presence of agglomerates (observed in

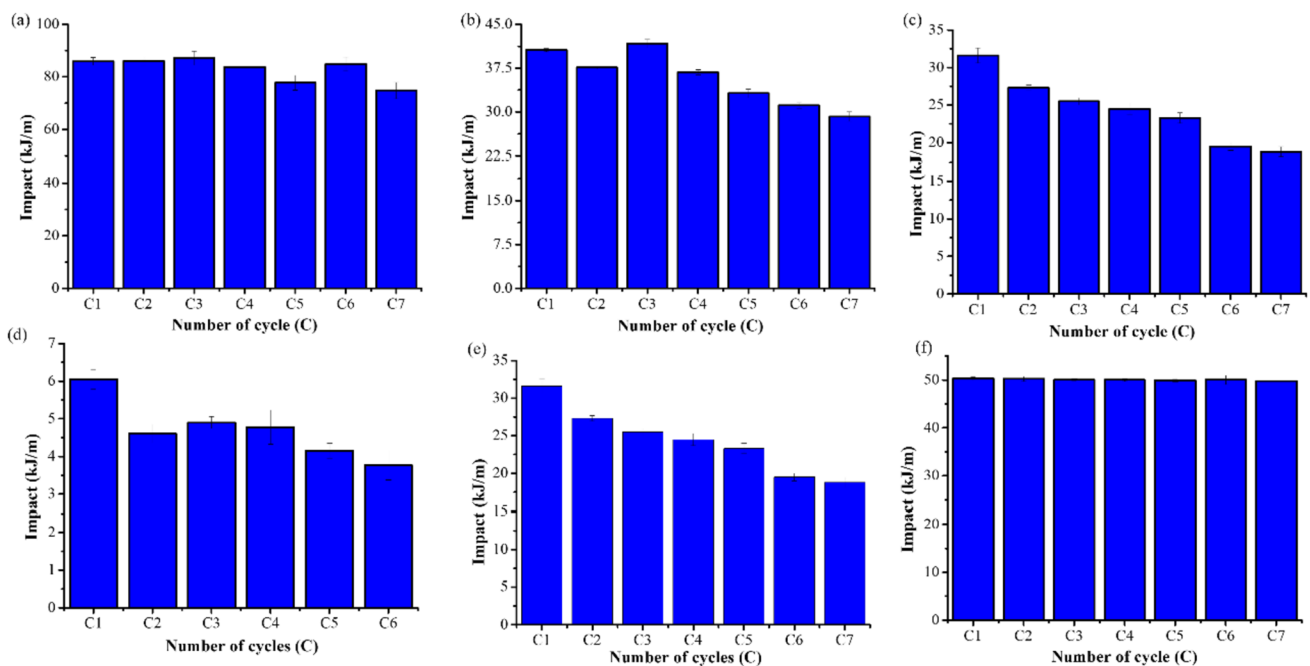


Fig. 2 Impact strength curves: **a** LDPE, **b** PBAT, **c** PBS, **d** PLA, **e** PBAT-PBS blend, and **f** PBAT-TPS composite after subjected to several reprocessing cycles

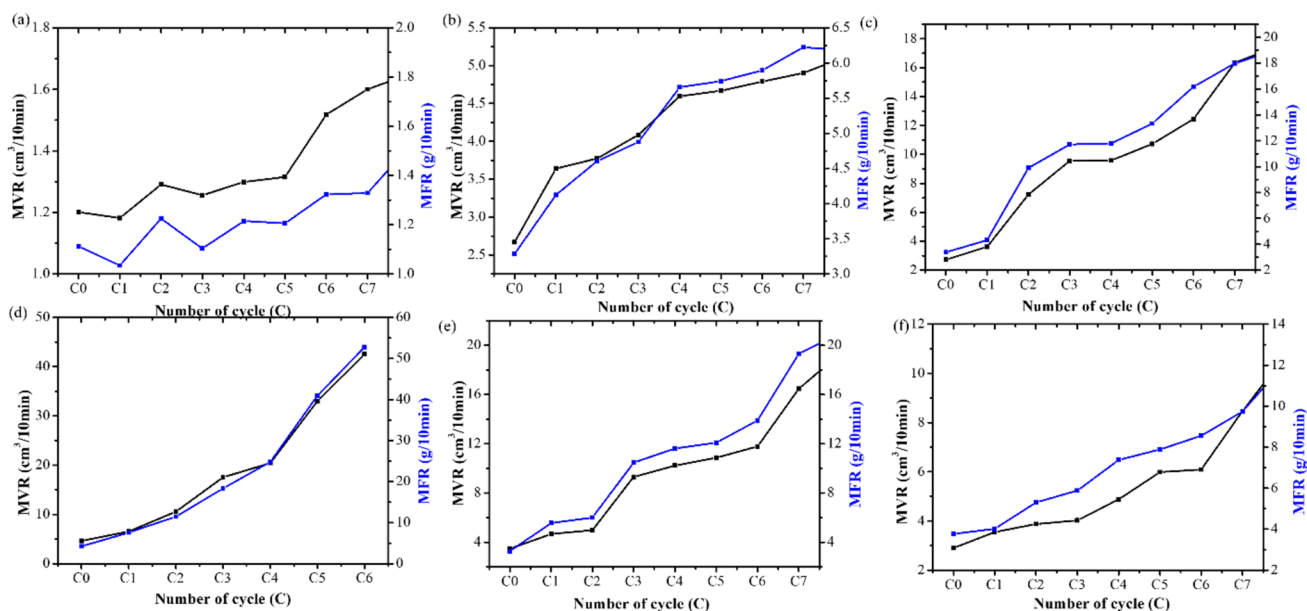


Fig. 3 MFI and MVR plots of **a** LDPE, **b** PBAT, **c** PBS, **d** PLA, **e** PBAT-PBS, and **f** PBAT-TPS after submitted to several processing cycles

SEM images). Additionally, the changes of MFI results did not give much effect in the mechanical properties due to bulk properties dynamic loading in the bond strength at elevated temperature. Instead, the changes of melt strength and viscosity occur mainly in the molecular level degradation when it is molten stage. This allowed good mechanical properties manifested by the tensile and impact strength results, due to enhanced stress transmission between the phases [39]. The MVR and MFR after the last reprocessing cycle were $50.4 \text{ cm}^3/10 \text{ min}$ and $53.2 \text{ g}/10 \text{ min}$ for PLA, $18.4 \text{ cm}^3/10 \text{ min}$ and $18.8 \text{ g}/10 \text{ min}$ for PBS, and $20.1 \text{ cm}^3/10 \text{ min}$ and $20.1 \text{ g}/10 \text{ min}$ for PBAT-PBS. Thus, they were not processable beyond these values.

DSC Analysis

The DSC curves and T_c , T_m , ΔH_c , ΔH_m and X_c values of LDPE, PBAT, PBS, PLA, PBAT-PBS, PBAT-TPS are represented in Fig. 4 and Table 1. LDPE results show small changes on the T_c , T_m , ΔH_c , ΔH_m and X_c values during multiple melt extrusion cycles, illustrating that minor thermal degradation incurred by the petroleum-based polymer. PBAT results (Table 1; Fig. 4b) show an increase in the crystallization temperature, T_c , from 69.87 to 78.12°C from the first to the seventh reprocessing cycle. Additionally, T_m proceeded to be slightly affected by the reprocessing since it increased from 121.13°C to 123.66°C , with no significant changes in crystallinity between the first and the seventh extrusion cycle. The observed results could be due to the degradation of unstable low molecular weight compounds

in the polymer matrix, which leads to an increase in thermal stability due to bulk molecules in the polymer matrix. On the other hand, the reprocessing effect on the PBS showed significant changes on the thermal properties, where the cold crystallization temperature decreased with an increasing number of reprocessing cycles. The increase of the cold-crystallization enthalpy of PBS indicates that thermo-mechanical degradation occurred as a result of chain scission mechanisms induced by multiple reprocessing, leading to low molecular weight compounds, with enhanced mobility and an ordered structure, thus, increased crystallinity, X_c [25, 40, 41]. *Bruster et al.* [25] reported similar behaviour when plasticised PLA was recycled for multiple times. The authors further correlated this behaviour to the decrease in tensile strength and these results were consistent with the observations of our study. Interestingly, Fig. 4d; Table 1 show that while the cold crystallization temperatures of PLA also decreased with increasing reprocessing cycles indicating polymer degradation due to chain scission mechanism, the cold crystallization enthalpy and the melting enthalpy were the same for all reprocessing cycles. *Akesson et al.* [26] observed the same trend and hypothesized that the unchanged ΔH_c and ΔH_m is because the amorphous regions of the semi-crystalline PLA are sensitive to hydrolytic degradation as they are water soluble and as such, experience thermomechanical degradation. In contrast, the crystalline regions are more resistant to thermomechanical degradation (Fig. 4d), thereby leading to unchanged values of ΔH_c and ΔH_m . The results of PBAT-PBS blend (Fig. 4e; Table 1), show that T_c and ΔH_c are increasing with the increasing number of reprocessing cycles. The increase in crystallinity

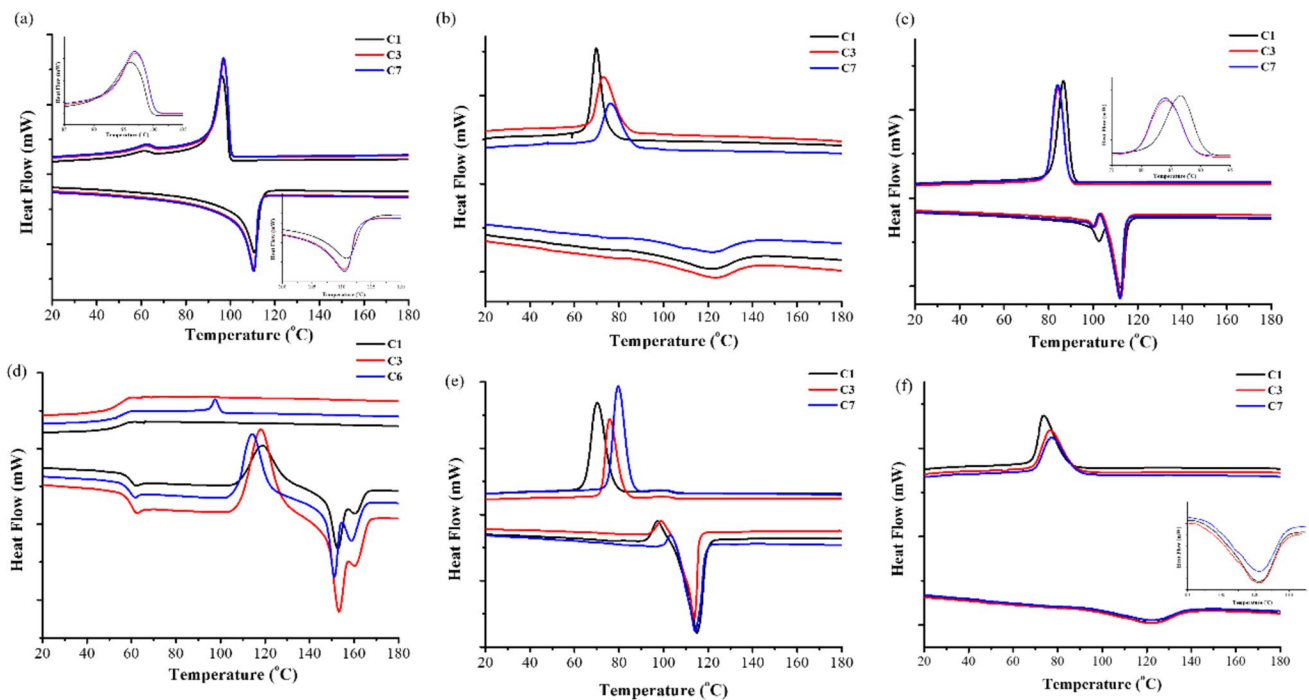


Fig. 4 DSC plots: **a** LDPE, **b** PBAT, **c** PBS and **d** PLA, **e** PBAT-PBS, and **f** PBAT-TPS after submitted to several processing cycles

enthalpy is mainly due to the thermomechanical degradation of neat PBS. This mechanism is slightly stabilized by the presence of PBAT on the microstructure of the matrix and it was manifested by the decrease in the crystallinity of the blend. However, further changes resulting from stress-induced melting and recrystallization from reprocessing were proposed to be responsible for the deformation process shown by the decrease in the T_m of the blend. This result suggests that the average lamellar thickness of the semi-crystalline polymer blend is decreasing [37, 42]. The change in the lamellar thickness indicates that the 50/50 ratio of the PBS-PBAT blend could not withstand the multiple reprocessing cycles, and as such, the mechanical properties (tensile strength, break-at-strain, impact, and MFI) were severely affected by recycling. The thermal properties of PBAT-TPS biocomposite were the most stable among other biopolymers, as demonstrated by the small changes in the DSC profile (Fig. 4f).

Thermogravimetric Analysis (TGA)

The effect of mechanical recycling on the thermostability of LDPE, PBAT, PBS, PLA, PBAT-PBS, and PBAT-TPS was analyzed by TGA under a nitrogen atmosphere. Comparative derivative thermogravimetric (DTG) curves are displayed in Fig. 5 and Table 1 also include T_{onset} and T_{max} results. All the test sample's thermogram results showed a general weight loss of $\sim 99.98\%$, regardless of the sample matrix and the

effect of reprocessing cycles. The T_{onset} of LDPE from the first to the seven reprocessing cycles decreased from $331.88\text{ }^\circ\text{C}$ to $321.17\text{ }^\circ\text{C}$, while T_{max} increased from $376.43\text{ }^\circ\text{C}$ to $397.38\text{ }^\circ\text{C}$. The results indicate that LDPE could have experienced slight thermal-oxidative attack during processing. *Holmstrom et al.* [43], reported that at elevated temperature the presence of oxygen, however small ($< 1.16\%$), can cause polymers like LDPE to experience thermal-oxidative reaction as processing occurs. This observation is also evidenced by the appearance of shoulder peaks (Fig. 5a), indicating generation of smaller molecules. However, the thermo-oxidative degradation does not affect the overall properties of the petroleum-based polymers since it is infinitesimally small. The difference in the T_{onset} of PBAT, PBS, PLA, and PBAT-PBS blend, between the first and seventh cycle, were $6.57\text{ }^\circ\text{C}$, $3.43\text{ }^\circ\text{C}$, $3.88\text{ }^\circ\text{C}$, and $0.57\text{ }^\circ\text{C}$, respectively, showing good thermal stability. PBAT-PBS thermograms (Fig. 5e) after the first cycle exhibited a single maximum degradation peak, at $393.53\text{ }^\circ\text{C}$, illustrating the miscibility between PBAT and PBS. However, as reprocessing cycles increased, the two biopolymers started to separate from each other, this is manifested by the two maximum degradation peaks. PBAT-TPS biocomposite curve (Fig. 5f) show that the thermal degradation followed a three-step process. The first step is attributed to the degradation of TPS along with the removal of moisture, and volatile compounds and it is characterized as peak at $308.14\text{ }^\circ\text{C}$. Then the second step is of the low molecular weight PBAT chains, with a T_{max} at

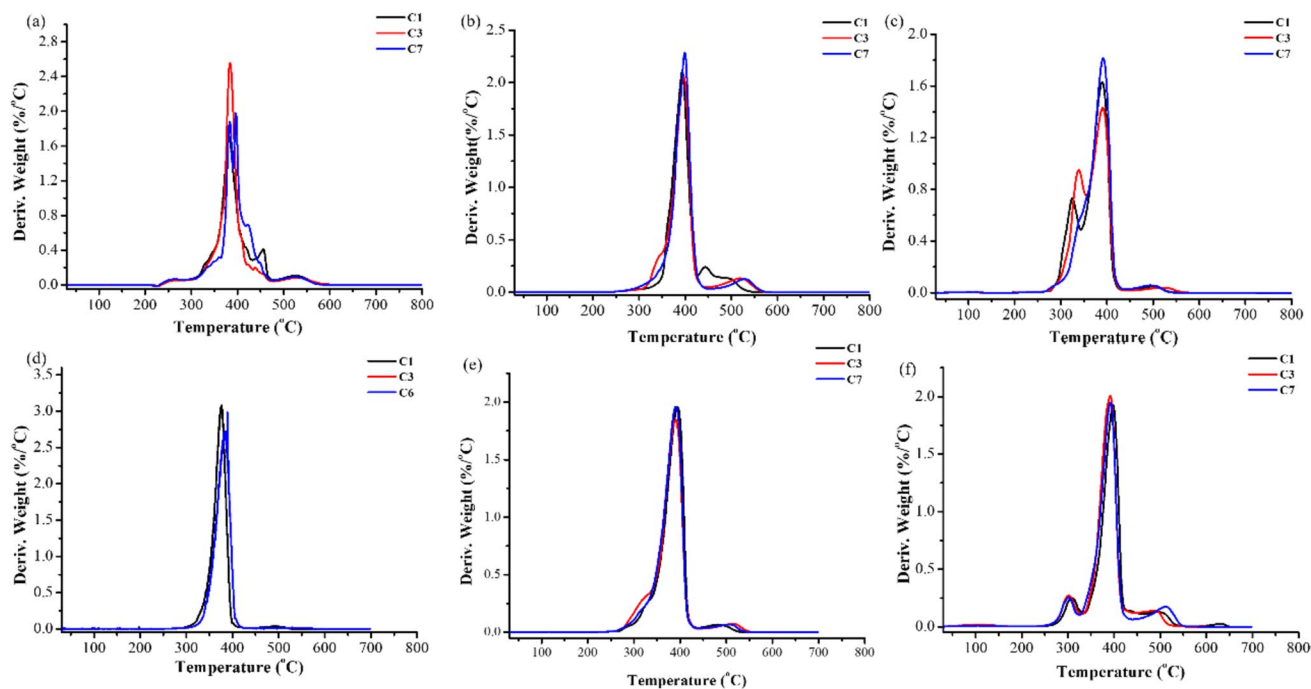


Fig. 5 DTG plots: **a** LDPE, **b** PBAT, **c** PBS and **d** PLA, **e** PBAT-PBS, and **f** PBAT-TPS after submitted to several processing cycles

396.52 °C. Finally, the third thermal event is of high molecular weight PBAT chains, characterized as peak at 491.36 °C. The onset degradation of the biocomposite decreased from 297.45 to 2847 °C, this is primarily as a results of the degradation TPS.

DMA Analysis

The dynamic mechanical analysis gives very important information on the modulus values concerning temperature changes during testing. The storage modulus and the loss factor, ($\tan \delta$) with respect to temperature plots at 10 Hz are shown in Figs. 6 and 7, respectively. Storage modulus and T_g (Figs. 6a and 7a) of LDPE results show that the seven melt-extrusion reprocessing cycles have an insignificant effect on the viscoelastic properties of the petroleum-based polymer. Figure 6b displays a slight increase in the storage modulus of neat PBAT in the glassy state as the reprocessing cycle increases. The observation is ascribed to the degradation of unstable low molecular weight compounds in the polymer matrix, as also observed in DSC analysis [12, 44]. There were no significant changes on the storage moduli above glass transition temperatures (rubbery region) as reprocessing cycles progressed. This indicates that reprocessing has an insignificant effect on the viscous properties of PBAT, which shows the stability of the material. The $\tan \delta$ curves, Fig. 7b, show a minor effect of reprocessing on the glass transition temperature of PBAT as illustrated by the prominent peak just below -20 °C. Multiple extrusion

had a different impact on the thermomechanical properties of PBS, as shown in Fig. 6c, where the storage modulus decreased significantly in both the glassy and rubbery state from the neat to the reprocessed PBS materials. The results suggest a decline in the molecular weight during reprocessing cycles, and the loss of modulus (E'') confirms that the viscous contribution of the main chain of macromolecules was significant. Similar results were observed in a study by *Shojaeiarani et al.* [45]. The authors monitored the deterioration in the physicomechanical and thermal properties of biopolymers due to reprocessing. They reported that both PLA and PHBV storage moduli were reduced throughout the entire temperature range due to the reduction of molecular weight. The T_g of PBS was not affected by reprocessing as the intense broad peak on the $\tan (\delta)$ curves (Fig. 7c) did not shift. In the case of PLA, Figs. 6d and 7d show that the storage modulus decreased, and T_g shifted from 70 °C to 75 °C as reprocessing cycles increased, respectively.

Before reprocessing the blend of PBAT-PBS exhibited a higher storage modulus than neat PBAT and PBS, confirming that blending the two biopolymers increased the rigidity of the polymer matrix and thus restricted the molecular movements of the polymers when force was applied. After reprocessing, a decrease of the storage moduli at both the glassy and the rubbery state of the polymer was observed, illustrating the overall effect of PBS on the blend. Additionally, only one prominent peak was observed on the $\tan (\delta)$ curves (Fig. 7e), showing the miscibility of PBAT and PBS polymers in the blend. Finally, Fig. 6f shows higher storage

Table 1 DSC and TGA data summary

Material	DSC						TGA	
	Cycle	T _c (°C)	ΔH _c (J/g)	T _m (°C)	ΔH _m (J/g)	X _c (%)	T _{5%} (°C)	T _{max} (°C)
LDPE	1	96.50	70.90	110.78	110.52	38.38	331.88	376.43
	3	97.35	77.22	110.00	110.51	38.37	327.12	387.21
	7	97.33	75.15	110.00	109.82	38.13	321.17	397.38
PBAT	1	69.87	14.7	121.13	10.19	8.94	355.00	393.57
	3	73.46	15.45	121.44	10.99	9.64	334.49	395.14
	7	78.12	12.65	123.66	9.73	8.53	348.43	396.37
PBS	1	86.25	60.25	104.49	1.98	40.21	307.99	390.06
	3	83.55	67.54	102.87	6.24	46.75	312.61	390.05
	7	83.25	88.46	103.07	6.44	62.18	311.42	390.67
PLA	1	118.87	28.80	152.63	35.49	37.88	333.67	372.27
	3	117.75	31.05	152.76	36.17	38.60	339.88	384.90
	6	113.87	29.30	150.70	31.60	33.73	337.55	380.22
PBAT-PBS	1	70.25	49.69	114.80	70.02	61.42	322.31	394.82
	3	76.17	53.91	113.56	69.51	60.97	314.19	393.50
	7	80.92	54.07	113.82	59.41	52.11	321.74	397.39
PBAT-TPS	1	73.75	15.03	122.28	10.16	8.91	297.45	308.14
	3	73.79	14.56	121.6	11.44	10.04	301.47	311.33
	7	77.99	12.81	125.19	6.20	5.44	284.70	313.66
Neat TPS	0	–	–	–	–	–	128.44	309.74

of modulus of PBAT-TPS composite as compared to neat PBAT. This is an attribute to the addition of TPS which possesses strong hydrogen bonds that result in difficulty of movement of the molecular chains. However, since the composite is largely made up of PBAT, the overall reprocessing effect behaves like neat PBAT, where only the glassy state is affected by reprocessing, while the rubbery state is insignificantly affected (Figs. 6f and 7f).

FTIR Studies

Figure 8 presents the FTIR spectra of LDPE, PBAT, PBS, PLA, PBAT-PBS blend, and PBAT-TPS composite during the multiple reprocessing cycles. The LDPE characteristic peaks observed from Fig. 8a are the intense asymmetric and symmetric C–H peaks at 2914 cm⁻¹ and 2896 cm⁻¹, respectively, with the moderate to small peaks of methyl and methylene C–H peaks at 1467 cm⁻¹ and 728 cm⁻¹, respectively.

Figure 8a also shows no change in the chemical nature of the polyolefin as reprocessing cycles progressed. The spectra of Fig. 8b highlights the characteristic bands of PBAT; the main peaks were found in the region of 3000–2800 cm⁻¹, 1750–1700 cm⁻¹, 1500 cm⁻¹, 1420–1250 cm⁻¹, 1100 cm⁻¹, 1000 cm⁻¹, 950 cm⁻¹ and 730 cm⁻¹. These peaks represent asymmetric and symmetric stretching vibrations of the CH₂ groups, C=O stretching vibration, skeleton vibration of the benzene ring, trans –CH₂– plane bending vibration, symmetric stretching vibration of C–O, bending vibration absorption, symmetric stretching vibration of trans C–O and bending vibration absorption of CH-plane of the benzene ring, respectively [46, 47]. No significant changes in the chemical structure of PBAT can be observed as a function of the processing cycle since the same bands are observed at the same wavenumbers with the same intensity. PBS spectrum, displayed by Fig. 8c, shows the characteristic groups of the polymer at 2963 cm⁻¹, 2921 cm⁻¹, 1710 cm⁻¹ and 1046 cm⁻¹

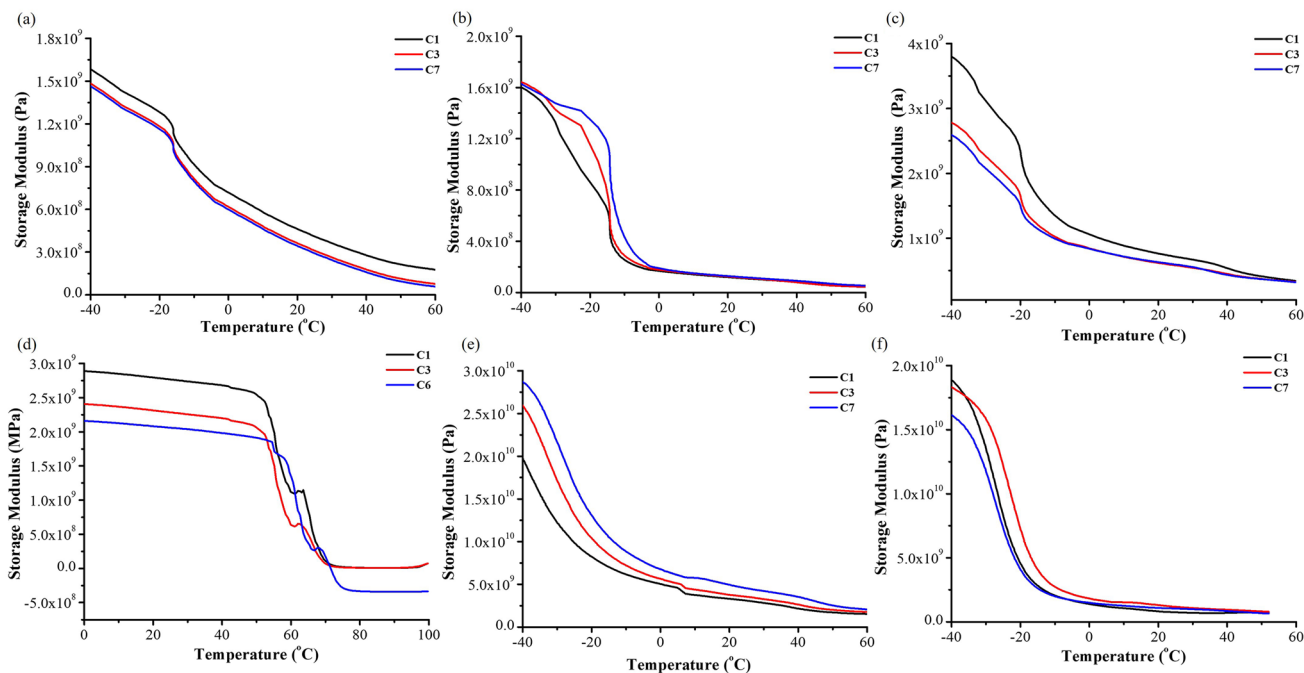


Fig. 6 Storage Modulus curves of **a** LDPE, **b** PBAT, **c** PBS, **d** PLA, **e** PBAT-PBS, and **f** PBAT-TPS after submitted to several processing cycle

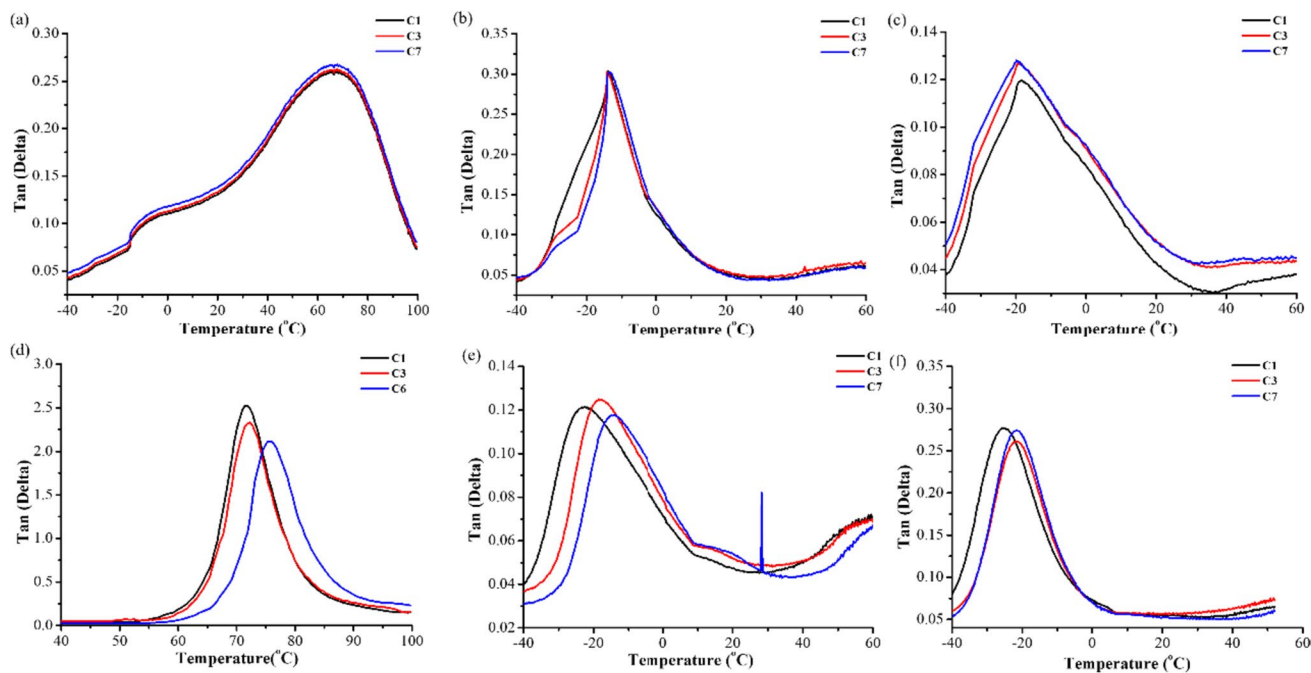


Fig. 7 Loss factor curves ($\tan\delta$) of **a** LDPE, **b** PBAT, **c** PBS, **d** PLA, **e** PBAT-PBS, and **f** PBAT-TPS after submitted to several processing cycles

which are attributed to the $-\text{CH}$ stretching, $\text{C}-\text{H}$ stretching vibration, $\text{C}=\text{O}$ stretching vibration and the stretching of the $-\text{C}-\text{O}-\text{C}$ respectively. While the peak at 1155 cm^{-1} is assigned to the ester linkages of PBS [48, 49]. Likewise, it is highlighted, that the multiple heating cycles did not

change the functional groups of the PBS polymer. PLA spectrum demonstrates the typical bands; the modes centered at 2997 cm^{-1} , 2946 cm^{-1} , 1456 cm^{-1} , and 1382 cm^{-1} are attributed to $-\text{CH}_3$ stretching, the band at 1750 cm^{-1} is associated with $\text{C}=\text{O}$ stretching, the signal at 1225 cm^{-1}

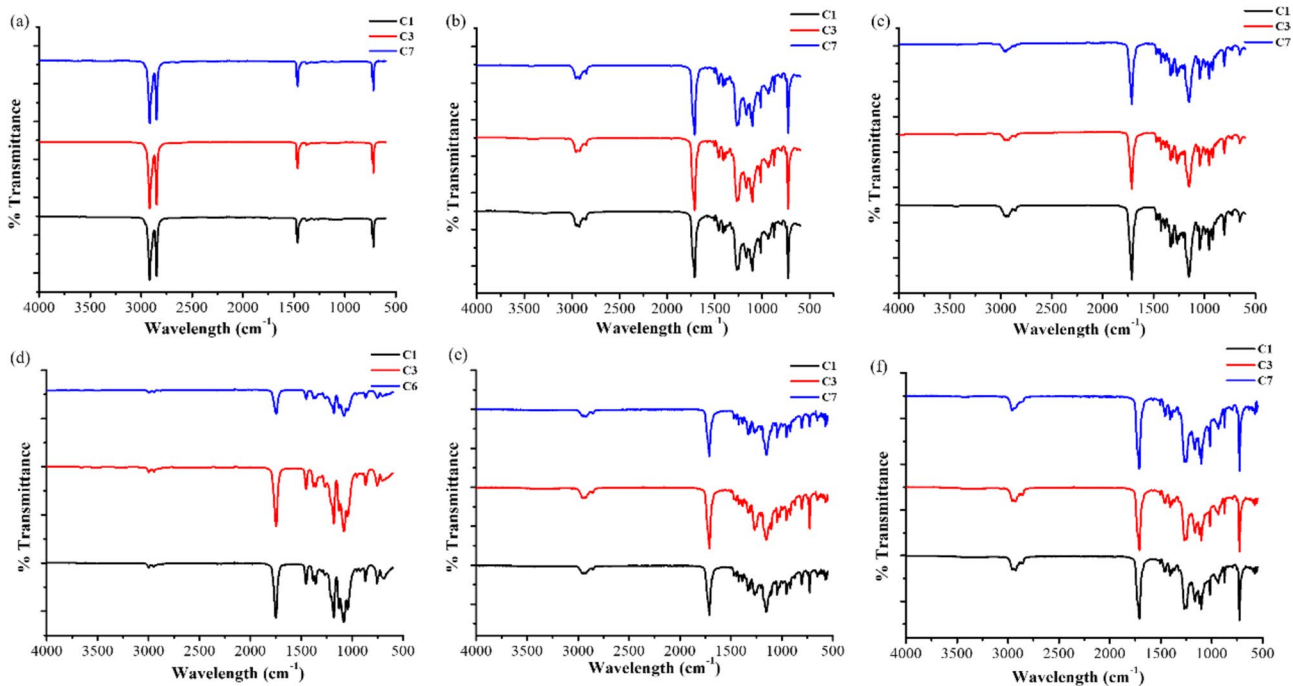


Fig. 8 FTIR spectrum of **a** LDPE, **b** PBAT, **c** PBS and **d** PLA, **e** PBAT-PBS blend, and **f** PBAT-TPS after submitted to several processing cycle

is associated with C=O bending, the band at 1049 cm^{-1} is associated with -OH bending, and those at 956 cm^{-1} and 921 cm^{-1} are attributed to -C-C stretching [50]. The lack of appearance of the hydroxyl and carbonyl terminated characteristic group as reprocessing cycle increased implies that trans-esterification and homolytic chain scission could be the degradation pathways which leads to the formation of cyclic oligomers instead [4, 23].

In the case of PBAT-PBS, the spectra (Fig. 8e) showed similar characteristic functional groups with those of neat PBS and PBAT. However, the intensities of the PBAT-PBS functional groups were less in comparison to neat PBAT and PBS, where the absorption band at wavenumber 1710 cm^{-1} corresponds to C=O stretching peaks. There was a slight shift of the characterization peaks of PBAT-PBS, which is attributed to the presence of a PBS conjugation. It is worth noting that there were no changes in the chemical nature of the PBAT-PBS blend and PLA initially; however, from the fifth and sixth cycle, there was a noticeable change in the carbonyl regions, where a decrease in the intensity of the carbonyl peak implied that the intense force exerted onto the blend during mechanical recycling promoted the cleavage of the C-H bonds belonging to the tertiary carbons, generating carbon-centered radicals that break the macromolecules and thereby encountering a chain-scission mechanism. The FTIR spectra of PBAT-TPS biocomposite are shown in Fig. 8f. The C=O characteristic peak was observed to have moved slightly to a lower wavenumber, i.e., at 1700 cm^{-1} ; the asymmetric/symmetric C-H stretched and C-O-C stretch were

observed at 2949 cm^{-1} , 2852 cm^{-1} , and 1246 cm^{-1} , respectively. The effect of repeated mechanical processing on the chemical properties of the biocomposite is not observed. Overall, multiple reprocessing did not show any oxidative and hydrolytic degradation effect on all the tested samples, and this is similar to other literature reports [37, 51].

SEM Analysis

Scanning electron microscopy (SEM) was used to analyze the impact of reprocessing cycles on the morphology of the LDPE, PBAT, PBS, PLA, PBAT-PBS blend and PBAT-TPS biocomposite. Figure 9 depicts two SEM images for each sample after the first and sixth or seventh cycle. The cross-section fracture image of LDPE 1 appears to have homogenous smooth morphology, after the seventh melt-extrusion cycle, the surface exhibit homogeneous grooves on the surface, could highlight the direction of the tensile pull test but the surface still looks undamaged, indicating that reprocessing had very little effect on the morphological properties of LDPE. PBAT 1 micrograph revealed a textured surface with multiple roughly spherical micro-structured domains, showing the complex and heterogeneous structural arrangements of PBAT as well as its ductile behavior upon fracture [52]. Interestingly, after the seven-reprocessing cycle, the surface of PBAT appears to be clear, smooth with a more homogeneous continuous surface. This may be attributed to the degradation of low molecular agglomerates because of shear stress and

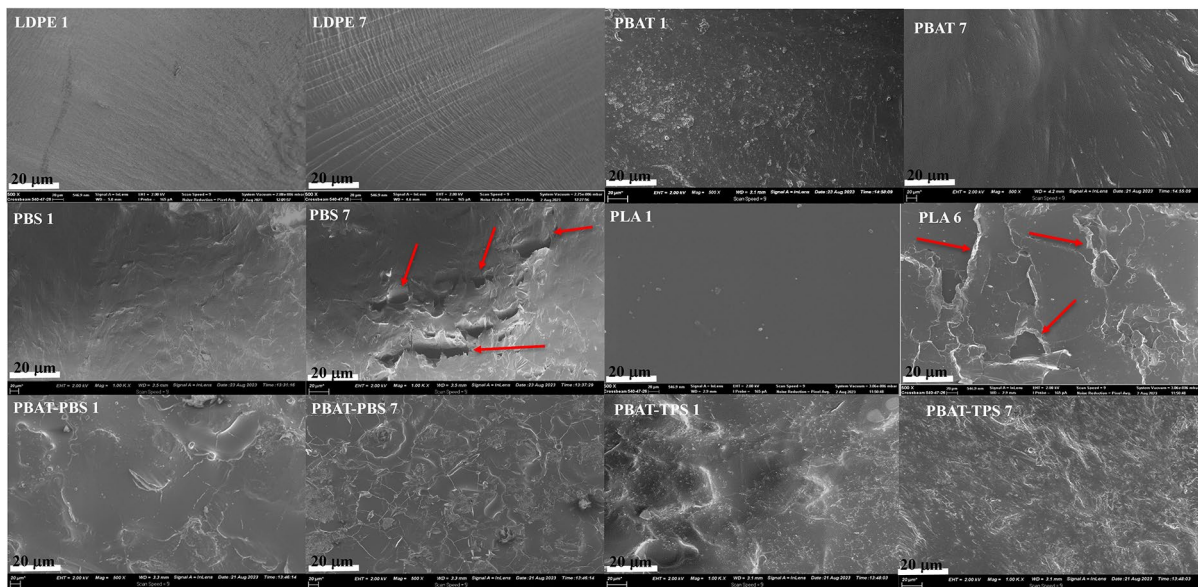


Fig. 9 SEM images of LDPE, PBAT, PBS, PLA, PBAT-PBS blend, and PBAT-TPS after the first and seventh processing cycle

temperature, thereby leading to a more thermally stable bulky polymer matrix as observed in the DSC analysis. The micrograph of PBS 1 highlights a smoother and thick textured surface, however, after the seven-reprocessing cycle, PBS surface exhibits a rough texture with very noticeable voids, illustrating the drastic effect of multiple reprocessing of the biopolymer. PLA 1 shows a smooth and thin textured surface morphology, this then changes after the sixth cycle, where PLA appears to have cracks, delaminated sections, and pits. Indicating the destruction of PLA morphology because of thermomechanical degradation and relates to poor mechanical properties, like PBS [53].

The morphology of neat PBAT-PBS is characterized by the ductile, thick textured continuous heterogeneous surface with granule-like spots, granting the material a rough exterior character. After the seventh cycle, the blend appears to have several sharp cracks and fractures all over the surface, clearly indicating the effect of the thermo-mechanical stress during reprocessing and this conforms the decline in the overall mechanical properties of the biopolymer blend. Intriguingly, the morphology of PBAT-TPS biocomposite depicts a very rough surface with sharp protruding strand-like spots all over the matrix, which can be attributed to partial miscibility of TPS on the biopolymer matrix. After the seventh reprocessing cycle, the surfaces still have a rough character but it is more evenly dispersed, and reprocessing appears to have improved the miscibility of TPS on the PBAT matrix as indicated by the replacement of sharp strands-like spots with a more thick-greasy ductile like texture rendering the biocomposite with enhanced mechanical properties compared to neat PBAT,

similar observations were reported by *Finnerty et al.* [54] and *Nayak et al.* [55].

Conclusion

The mechanical recyclability of PBAT, PBS, PLA, PBAT-PBS blend, and PBAT-TPS biocomposite was investigated by carrying out seven melt extrusion cycles using twin-screw extrusion and injection molding processing techniques and monitoring the mechanical, thermal, physical, morphological, and chemical changes at each melt extrusion cycle. The results obtained revealed that shear stress and elevated temperature induced chain scission, evidenced by the increase in the melt flow index of PBS, PLA, and PBAT-PBS; this correlated to the reduction of molecular weight, which in turn enhanced the mobility and ordered structure of polymer chains, thus, increased crystallinity, X_c and storage modulus. Consequently, the increase in crystallinity led to a stiffer polymer, manifested by decreased impact energy and strain-at-break. For example, unprocessed PBS's MVR and MFR values increased from 2.7 cm³/10min and 3.3 g/10min to 20.8 cm³/10min and 19.6 g/10min by the seventh cycle, respectively. This was accompanied by a decrease in T_c from 86.25 °C to 83.25 °C and an increase of ΔH_m from 60.25 J/g to 88.46 J/g. While the impact energy reduced from 31.6 kJ/m to 16.4 kJ/m, and the strain at break decreased from 1013.0 to 63.9%, respectively. These changes were evidence of thermomechanical degradation and were confirmed by micro-morphological changes from relatively smooth surfaces to rough, cracked surfaces. Similar observations were deduced for PLA and PBAT-PBS. The results

showed that PBS and PBAT-PBS can only be mechanically recycled seven times, and PLA can be recycled six times.

The study further showed that PBAT and PBAT-TPS were melt-extrudable throughout the seven cycles with slight melt flow changes, indicating high potential mechanical recyclability of the biopolymer and biopolymer composite. The resistance ability of PBAT thermomechanical properties during several reprocessing cycles is mainly attributed to the aromatic content within the biopolymer chain. Additionally, TPS reinforced PBAT matrix exhibited improved mechanical and thermal properties. In summary, PBAT and PBAT-TPS biocomposite were the best-performing biopolymers in terms of multiple processabilities, and the performance of the biopolymers were comparable to LDPE. Thus, the order of mechanical recyclability of biopolymers is PBAT-TPS > PBAT > PBS > PBAT-PBS > PLA.

Author Contributions SM conceptualized, funding acquisition, and supervised. SM, OO, NN, and AM designed the methodology. NN carried out the primary investigation and wrote the main manuscript. JL Section 2.1.3 and 2.14 CM prepared Fig. 5, 6. SM, OO, NN, and AM validation, curation and visualization. All authors reviewed and agreed to the published version of the manuscript.

Funding Open access funding provided by Nelson Mandela University. The authors would like to acknowledge the financial support for this project via a CSIR Parliamentary Grant and the South African Department of Science and Innovation's Waste Research, Development, and Innovation (RDI) program.

Declarations

Competing Interests The authors declare no competing interests.

Open Access This article is licensed under a Creative Commons Attribution 4.0 International License, which permits use, sharing, adaptation, distribution and reproduction in any medium or format, as long as you give appropriate credit to the original author(s) and the source, provide a link to the Creative Commons licence, and indicate if changes were made. The images or other third party material in this article are included in the article's Creative Commons licence, unless indicated otherwise in a credit line to the material. If material is not included in the article's Creative Commons licence and your intended use is not permitted by statutory regulation or exceeds the permitted use, you will need to obtain permission directly from the copyright holder. To view a copy of this licence, visit <http://creativecommons.org/licenses/by/4.0/>.

References

- Al Hosni AS, Pittman JK, Robson GD (2019) Microbial degradation of four biodegradable polymers in soil and compost demonstrating polycaprolactone as an ideal compostable plastic. *Waste Manag* 97:105–114. <https://doi.org/10.1016/j.wasman.2019.07.042>
- Parida M, Shajkumar A, Mohanty S, Biswal M, Nayak SK (2022) Poly(lactic acid) (PLA)-based mulch films: evaluation of mechanical, thermal, barrier properties and aerobic biodegradation characteristics in real-time environment. *Polym Bull.* <https://doi.org/10.1007/s00289-022-04203-4>
- Thakur S, Chaudhary J, Sharma B, Verma A, Tamulevicius S, Thakur VK (2018) Sustainability of bioplastics: opportunities and challenges. *Curr Opin Green Sustain Chem* 13:68–75. <https://doi.org/10.1016/j.cogsc.2018.04.013>
- Scaffaro R, Maio A, Sutera F, ortunato Gulino E, Morreale M (2019) Degradation and recycling of films based on biodegradable polymers: a short review. *Polymers* 11:651. <https://doi.org/10.3390/polym11040651>
- Mtibe A, Motloug MP, Bandyopadhyay J, Ray SS (2021) Synthetic Biopolymers and Their Composites: Advantages and Limitations—An Overview. *Macromol Rapid Commun* 42:2100130. <https://doi.org/10.1002/marc.202100130>
- Fredi G, Dorigato A (2021) Recycling of bioplastic waste: A review. *Adv Ind Eng Polym Res* 4:159–177. <https://doi.org/10.1016/j.aiepr.2021.06.006>
- Geyer R, Jambeck JR, Law KL (2017) Production, use, and fate of all plastics ever made. *Sci Adv* 3:e1700782. <https://doi.org/10.1126/sciadv.1700782>
- Emadian SM, Onay TT, Demirel B (2017) Biodegradation of bioplastics in natural environments. *Waste Manag* 59:526–536. <https://doi.org/10.1016/j.wasman.2016.10.006>
- Van Rooijen EC, Miller SA (2022) A review of bioplastics at end-of-life: Linking experimental biodegradation studies and life cycle impact assessments. *Resour Conserv Recycl* 181:106236. <https://doi.org/10.1016/j.resconrec.2022.106236>
- Dilkes-Hoffman L, Ashworth P, Laycock B, Pratt S, Lant P (2019) Public attitudes towards bioplastics—knowledge, perception and end-of-life management. *Resour Conserv Recycl* 151:104479. <https://doi.org/10.1016/j.resconrec.2019.104479>
- Changwichan K, Silalertruksa T, Gheewala SH (2018) Eco-efficiency assessment of bioplastics production systems and end-of-life options. *Sustainability.* <https://doi.org/10.3390/su10040952>
- Gil-Castell O, Badia JD, Ribes-Greus A (2018) Suitability of blends from virgin and reprocessed polylactide: performance and energy valorization kinetics. *J Renew Mater* 6:370–382. <https://doi.org/10.7569/JRM.2017.634170>
- Georgousopoulou IN, Vouyiouka S, Dole P, Papispyrides CD (2016) Thermo-mechanical degradation and stabilization of poly(butylene succinate). *Polym Degrad Stab* 128:182–192. <https://doi.org/10.1016/j.polymdegradstab.2016.03.012>
- Ceretti DVA, Edeleva M, Cardon L, D'hooge DR (2023) Molecular pathways for Polymer Degradation during Conventional Processing, Additive Manufacturing, and mechanical recycling. *Molecules* 28:2344. <https://doi.org/10.3390/molecules28052344>
- Wu H, Lv S, He Y, Qu JP (2019) The study of the thermomechanical degradation and mechanical properties of PET recycled by industrial-scale elongation processing. *Polym Test.* <https://doi.org/10.1016/j.polymertesting.2019.04.029>
- Capone C, Di Landro L, Inzoli F, Penco M, Sartore L (2007) Thermal and mechanical degradation during polymer extrusion processing. *Polym Eng Sci* 47:1813–1819. <https://doi.org/10.1002/pen.20882>
- La Mantia FP, Morreale M, Botta L, Mistretta MC, Ceraulo M, Scaffaro R (2017) Degradation of Polymer blends: a brief review. *Polym Degrad Stab* 145:79–92. <https://doi.org/10.1016/j.polymdegradstab.2017.07.011>
- Vollmer I, Jenks MJF, Roelands MCP, White RJ, van Harmelen T, de Wild P, van der Laan GP, Meirer F, Keurentjes JTF, Weckhuysen BM (2020) Beyond mechanical recycling: giving New Life to Plastic Waste. *Angewandte Chemie - International Edition* 59:15402–15423. <https://doi.org/10.1002/anie.201915651>
- Schyns ZOG, Shaver MP (2021) Mechanical Recycling of Packaging Plastics: A Review. *Macromol Rapid Commun.* <https://doi.org/10.1002/marc.202000415>

20. Oliveira TA, Oliveira RR, Barbosa R, Azevedo JB, Alves TS (2017) Effect of reprocessing cycles on the degradation of PP/PBAT-thermoplastic starch blends. *Carbohydr Polym* 168:52–60. <https://doi.org/10.1016/j.carbpol.2017.03.054>
21. Resch-Fauster K, Klein A, Bles E, Feuchter M (2017) Mechanical recyclability of technical biopolymers: potential and limits. *Polym Test* 64:287–295. <https://doi.org/10.1016/j.polymertesting.2017.10.017>
22. Bourmaud A, Beaugrand J, Shah DU, Placet V, Baley C (2018) Towards the design of high-performance plant fibre composites. *Prog Mater Sci* 97:347–408. <https://doi.org/10.1016/j.pmatsci.2018.05.005>
23. Dedieu I, Peyron S, Gontard N, Aouf C (2022) The thermo-mechanical recyclability potential of biodegradable biopolyesters: Perspectives and limits for food packaging application. *Polym Test*. <https://doi.org/10.1016/j.polymertesting.2022.107620>
24. Bourmaud A, Åkesson D, Beaugrand J, Le Duigou A, Skrifvars M, Baley C (2016) Recycling of L-Poly-(lactide)-Poly-(butylene-succinate)-flax biocomposite. *Polym Degrad Stab* 128:77–88. <https://doi.org/10.1016/j.polymdegradstab.2016.03.018>
25. Brüster B, Addiego F, Hassouna F, Ruch D, Raquez JM, Dubois P (2016) Thermo-mechanical degradation of plasticized poly(lactide) after multiple reprocessing to simulate recycling: multi-scale analysis and underlying mechanisms. *Polym Degrad Stab* 131:132–144. <https://doi.org/10.1016/j.polymdegradstab.2016.07.017>
26. Åkesson D, Vriegnaud T, Tissot C, Skrifvars M (2016) Mechanical recycling of PLA filled with a high level of Cellulose Fibres. *J Polym Environ* 24:185–195. <https://doi.org/10.1007/s10924-016-0760-0>
27. Scaffaro R, Morreale M, Mirabella F, La Mantia FP (2011) Preparation and recycling of plasticized PLA. *Macromol Mater Eng* 296:141–150. <https://doi.org/10.1002/mame.201000221>
28. Badia JD, Strömberg E, Karlsson S, Ribes-Greus A (2012) Material valorisation of amorphous polylactide. Influence of thermo-mechanical degradation on the morphology, segmental dynamics, thermal and mechanical performance. *Polym Degrad Stab* 97:670–678. <https://doi.org/10.1016/j.polymdegradstab.2011.12.019>
29. Lopez JP, Girones J, Mendez JA, Puig J, Pelach MA (2012) Recycling ability of biodegradable matrices and their Cellulose-Reinforced composites in a Plastic Recycling Stream. *J Polym Environ* 20:96–103. <https://doi.org/10.1007/s10924-011-0333-1>
30. Bastarrachea L, Dhawan S, Sablani SS, Mah JH, Kang DH, Zhang J, Tang J (2010) Biodegradable poly(Butylene adipate-co-terephthalate) films incorporated with nisin: characterization and effectiveness against *Listeria innocua*. *J Food Sci*. <https://doi.org/10.1111/j.1750-3841.2010.01591.x>
31. Xu J, Guo B-H (2010) Microbial succinic acid, its polymer poly(butylene succinate), and applications. *Plastics from bacteria*. Springer, Berlin. https://doi.org/10.1007/978-3-642-03287-5_14
32. Herrera R, Franco L, Rodríguez-Galán A, Puiggali J (2002) Characterization and degradation behavior of poly(butylene adipate-co-terephthalate)s. *J Polym Sci A Polym Chem* 40:4141–4157. <https://doi.org/10.1002/pola.10501>
33. Lee SH, Lim SW, Lee KH (1999) Properties of potentially biodegradable copolyesters of (succinic acid-1,4-butanediol)/(dimethyl terephthalate-1,4-butanediol). *Polym Int* 48:861–867
34. Nagarajan V, Misra M, Mohanty AK (2013) New engineered biocomposites from poly(3-hydroxybutyrate-co-3-hydroxyvalerate) (PHBV)/poly(butylene adipate-co-terephthalate) (PBAT) blends and switchgrass: fabrication and performance evaluation. *Ind Crops Prod* 42:461–468. <https://doi.org/10.1016/j.indcrop.2012.05.042>
35. Bordes P, Pollet E, Avérous L (2009) Nano-biocomposites: biodegradable polyester/nanoclay systems. *Progress in Polymer Science (Oxford)* 34:125–155. <https://doi.org/10.1016/j.progpolymsci.2008.10.002>
36. Ferreira FV, Cividanes LS, Gouveia RF, Lona LMF (2019) An overview on properties and applications of poly(butylene adipate-co-terephthalate)-PBAT based composites. *Polym Eng Sci*. <https://doi.org/10.1002/pen.24770>
37. Wang K, Addiego F, Bahlouli N, Ahzi S, Rémond Y, Toniazio V, Muller R (2012) Analysis of thermomechanical reprocessing effects on polypropylene/ethylene octene copolymer blends. *Polym Degrad Stab* 97:1475–1484. <https://doi.org/10.1016/j.polymdegradstab.2012.05.005>
38. Delva L, Ragaert K, Degrieck J, Cardon L (2014) The effect of multiple extrusions on the properties of montmorillonite filled polypropylene. *Polym (Basel)* 6:2912–2927. <https://doi.org/10.3390/polym6122912>
39. de Carvalho MS, Azevedo JB, Barbosa JDV (2020) Effect of the melt flow index of an HDPE matrix on the properties of composites with wood particles. *Polym Test*. <https://doi.org/10.1016/j.polymertesting.2020.106678>
40. Rojas-González AF, Carrero-Mantilla JI (2015) Cinética de degradación térmica de poliácido láctico en múltiples extrusiones. *Ingeniería Y Universidad* 19:189–206. <https://doi.org/10.11144/Javeriana.iyu19-1.tdkp>
41. Agüero A, Morcillo MdelC, Quiles-Carrillo L, Balart R, Boronat T, Lascano D, Torres-Giner S, Fenollar O (2019) Study of the influence of the reprocessing cycles on the final properties of polylactide pieces obtained by injection molding. *Polymers*. <https://doi.org/10.3390/polym11121908>
42. Wang Y, Jiang Z, Fu L, Lu Y, Men Y (2014) Lamellar thickness and stretching temperature dependency of cavitation in semicrystalline polymers. *PLOS ONE*. <https://doi.org/10.1371/journal.pone.0097234>
43. Holmström A, Sörvik E (1974) Thermal degradation of polyethylene in a nitrogen atmosphere of low oxygen content. III. Structural changes occurring in low-density polyethylene at oxygen contents below 1.2%. *J Appl Polym Sci* 18:3153–3178. <https://doi.org/10.1002/app.1974.070181022>
44. Baghaei B, Skrifvars M, Berglin L (2013) Manufacture and characterisation of thermoplastic composites made from PLA/hemp co-wrapped hybrid yarn prepregs. *Compos Part A Appl Sci Manuf* 50:93–101. <https://doi.org/10.1016/j.compositesa.2013.03.012>
45. Shojaeiarani J, Bajwa DS, Rehovsky C, Bajwa SG, Vahidi G (2019) Deterioration in the physico-mechanical and thermal properties of biopolymers due to reprocessing. *Polymers*. <https://doi.org/10.3390/polym11010058>
46. de Freitas ALP, Tonini Filho LR, Calvão PS, de Souza AMC (2017) Effect of montmorillonite and chain extender on rheological, morphological and biodegradation behavior of PLA/PBAT blends. *Polym Test* 62:189–195. <https://doi.org/10.1016/j.polymertesting.2017.06.030>
47. Palsikowski PA, Kuchnier CN, Pinheiro IF, Morales AR (2018) Biodegradation in Soil of PLA/PBAT blends compatibilized with Chain Extender. *J Polym Environ* 26:330–341. <https://doi.org/10.1007/s10924-017-0951-3>
48. Muthuraj R, Misra M, Mohanty AK (2015) Hydrolytic degradation of biodegradable polyesters under simulated environmental conditions. *J Appl Polym Sci*. <https://doi.org/10.1002/app.42189>
49. Phua YJ, Chow WS, Mohd ZA, Ishak (2013) Reactive processing of maleic anhydride-grafted poly(butylene succinate) and the compatibilizing effect on poly(butylene succinate) nanocomposites. *Express Polym Lett* 7:340–354. <https://doi.org/10.3144/expresspolymlett.2013.31>
50. Scaffaro R, Maio A, Gulino FE, Di Salvo C, Arcarisi A (2020) Bilayer biodegradable films prepared by co-extrusion film

- blowing: Mechanical performance, release kinetics of an antimicrobial agent and hydrolytic degradation. *Compos Part A*. <https://doi.org/10.1016/j.compositesa.2020.105836>
51. Sarrionandia M, Lopez-Arraiza A, Aurrekoetxea J, Arostegui A (2009) Structure and mechanical properties of a talc-filled polypropylene/ethylene-propylene-diene composite after reprocessing in the melt state. *J Appl Polym Sci* 114:1195–1201. <https://doi.org/10.1002/app.30080>
 52. Nobile MR, Crocitti A, Malinconico M, Santagata G, Cerruti P (2018) Preparation and characterization of polybutylene succinate (PBS) and polybutylene adipate-terephthalate (PBAT) biodegradable blends. *AIP Conference Proceedings*. American Institute of Physics Inc, College Park,. <https://doi.org/10.1063/1.5046042>
 53. Azevedo JVC, Ramakers-Van Dorp E, Grimmig R, Hausnerova B, Möglinger B (2022) Process-Induced Morphology of Poly(Butylene Adipate Terephthalate)/Poly(Lactic Acid) Blown Extrusion Films Modified with Chain-Extending Cross-Linkers. *Polymers*. <https://doi.org/10.3390/polym14101939>
 54. Finnerty J, Rowe S, Howard T, Connolly S, Doran C, Devine DM, Gately NM, Chyzna V, Portela A, Bezerra GSN, McDonald P, Colbert DM (2023) Effect of Mechanical Recycling on the Mechanical Properties of PLA-Based Natural Fiber-Reinforced Composites. *J Compos Sci*. <https://doi.org/10.3390/jcs7040141>
 55. Nayak SK (2010) Biodegradable PBAT/Starch nanocomposites. *Polym Plast Technol Eng* 49:1406–1418. <https://doi.org/10.1080/03602559.2010.496397>

Publisher's Note Springer Nature remains neutral with regard to jurisdictional claims in published maps and institutional affiliations.

Authors and Affiliations

Nomvuyo Nomadolo^{1,2} · Asanda Mtibe¹ · Osei Ofosu^{1,3} · Caroline Mekoa¹ · John Letwaba¹ · Sudhakar Muniyasamy^{1,2}

✉ Sudhakar Muniyasamy
smuniyasamy@csir.co.za

¹ Centre for Nanostructures and Advanced Materials, Council for Scientific and Industrial Research (CSIR), Pretoria 0001, South Africa

² Department of Chemistry, Faculty of Sciences, Nelson Mandela University, Port Elizabeth 6000, South Africa

³ Department of Textile Science, Faculty of Sciences, Nelson Mandela University, Port Elizabeth 6031, South Africa